



ELSEVIER

Contents lists available at ScienceDirect

Solid State Electronics

journal homepage: www.elsevier.com/locate/sse

Design and fabrication of low power GaAs/AlAs resonant tunneling diodes

Mohamad Adzhar Md Zawawi^{a,*}, Mohamed Missous^b

^a School of Electrical and Electronic Engineering, Engineering Campus, Universiti Sains Malaysia, 14300 Nibong Tebal, Penang, Malaysia

^b School of Electrical and Electronic Engineering, University of Manchester, Sackville Street, Manchester M13 9PL, UK

ARTICLE INFO

Keywords:

GaAs
AlAs
Resonant tunneling diode
Oscillator
III-V compound semiconductor

ABSTRACT

A very low peak voltage GaAs/AlAs resonant tunneling diode (RTD) grown by molecular beam epitaxy (MBE) has been studied in detail. Excellent growth control with atomic-layer precision resulted in a peak voltage of merely 0.28 V (0.53 V) in forward (reverse) direction. The peak current density in forward bias is around 15.4 kA/cm² with variation of within 7%. As for reverse bias, the peak current density is around 22.8 kA/cm² with 4% variation which implies excellent scalability. In this work, we have successfully demonstrated the fabrication of a GaAs/AlAs RTD by using a conventional optical lithography and chemical wet-etching with very low peak voltage suitable for application in low dc input power RTD-based sub-millimetre wave oscillators.

1. Introduction

Over the past three decades, resonant tunneling diodes (RTD) have received a great deal of attention owing to its ability to generate a very high fundamental frequency well into the THz region. The monolithic integration of RTDs with an optimised oscillator circuit can potentially produce a compact solid-state continuous-wave (CW) terahertz source working at room temperature [1–3]. To date, the highest room temperature fundamental oscillation of up to 1.46 THz is achieved in highly-doped collector RTD [4]. The THz and sub-THz frequency facilitate the applications of radio astronomy, medical imaging, surveillance and security, atmospheric and environmental monitoring and also in telecommunication [5].

There are several material systems that can be used to construct resonant tunneling diodes. However, group III-IV compound semiconductor materials are generally mature in terms of growth technique and technology. For GaAs-based resonant tunneling diode, there are basically two options for the barrier epi-layer material. One, is to employ an Al_xGa_{1-x}As layer and the other is to use the binary AlAs. In terms of conduction band offset, the former has a lower barrier that results in a higher over-the-barrier leakage current. While the GaAs/AlAs system has ~1.0 eV conduction band offset at the Γ - Γ point, this implies a higher peak to valley current ratio (PVCR) through suppression of the thermionic current component. The use of an AlAs barrier as compared to Al_xGa_{1-x}As is known to also reduce alloy scattering. Lower temperature growth of AlAs also helps to reduce the risk of dopant diffusion into the active region.

Resonant tunneling diode with GaAs/AlAs material system had been

introduced for the first time by Tsuchiya et al. in 1985 [6]. The electrodes were highly doped and negative differential resistance (NDR) at room temperature was observed. In general, improvement on peak current density is attributed to the increased transmission probability. The improvement in peak-to-valley current ratio (PVCR) is due to the reduction of alloy scattering in AlAs barrier. This lead to the reduction in leakage current components. In addition, the increased barrier height reduces unwanted tunneling current through higher lying resonant level.

In this work, conventional GaAs/AlAs RTDs were fabricated with careful attention given on the growth condition in return for high quality junction interfaces. As a result, the peak current occurs at a very low voltage. This feature is vital especially in battery-operated low input dc power THz sources.

2. Experimental

2.1. Epitaxial layer structure

The GaAs/AlAs resonant tunneling double barrier structure under study was grown by using an in-house RIBER V100H solid-source molecular beam epitaxy (MBE) system. This particular wafer was given the code XMBE#66 with epitaxial layer structures as listed in Table 1.

From bottom to top, the sample is grown on a (1 0 0)-oriented semi-insulating GaAs substrate followed by a GaAs buffer layer to provide some margins especially during device isolation. The thick buffer (1320 Å) provides excellent crystal quality. The GaAs emitter layer is heavily n-doped with silicon (Si) dopants of $3.0 \times 10^{18} \text{ cm}^{-3}$. This highly

* Corresponding author.

E-mail address: adzhar@usm.my (M.A. Md Zawawi).

Table 1
Epitaxial layer structure of the GaAs/AlAs resonant tunneling diode used in this work.

Layer	Material	Doping (cm^{-3})	Thickness (\AA)
Collector	GaAs(n++)	7.0×10^{18}	5000
Spacer	GaAs	Undoped	150
Barrier	AlAs	Undoped	17
Quantum Well	GaAs	Undoped	65
Barrier	AlAs	Undoped	17
Spacer	GaAs	Undoped	350
Emitter	GaAs(n++)	3.0×10^{18}	8000
Buffer	GaAs	Undoped	1320
Substrate	GaAs		

doped layer will facilitate good ohmic contact. An undoped spacer layer is grown before the first barrier. From a growth perspective, the benefit of having a spacer layer is to suppress dopant diffusion into the subsequent layer during high temperature growth. The double barrier single quantum well (DBQW) in the middle structure consist of a narrow band-gap GaAs sandwiched in between two higher band-gap AlAs materials. Finally, a highly doped, degenerate collector layer on top of the second spacer completed the resonant tunneling device structure. The wafer is diced into $15 \text{ mm} \times 15 \text{ mm}$ tiles for easy handling and processing. The details on growth condition and atomic layer precision control of the MBE system used in this work are described by P. Dasmahapatra et al. [7].

2.2. Fabrication process

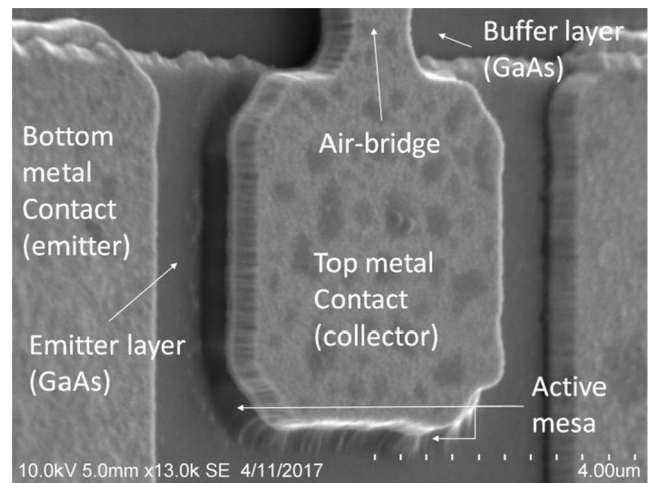
The process started with sample cleaning by using N-Methyl Pyrrolidone (NMP), Acetone and Propan-2-ol (IPA) consecutively for 5 min each in order to remove both organic and in-organic contaminants. Except NMP, both Acetone and IPA processing are performed in an ultrasonic bath to remove particles more effectively.

The top down processing approach is then followed by patterning the sample with AZnLOF2020 negative photoresist. By using a conventional i-line optical lithography, areas of $2 \mu\text{m} \times 2 \mu\text{m}$, $3 \mu\text{m} \times 3 \mu\text{m}$, $4 \mu\text{m} \times 4 \mu\text{m}$, $5 \mu\text{m} \times 5 \mu\text{m}$ and $6 \mu\text{m} \times 6 \mu\text{m}$ are defined as the collector top metal contact. This collector contact is connected to the bond pad through an air-bridge with dimensions of $1 \mu\text{m}$ (width) \times $5 \mu\text{m}$ (length) on the same plane. An alloyed ohmic contact is established by thermal evaporation of AuGe, Ni and followed by Au with respective thicknesses of 50 nm, 13 nm and 200 nm each.

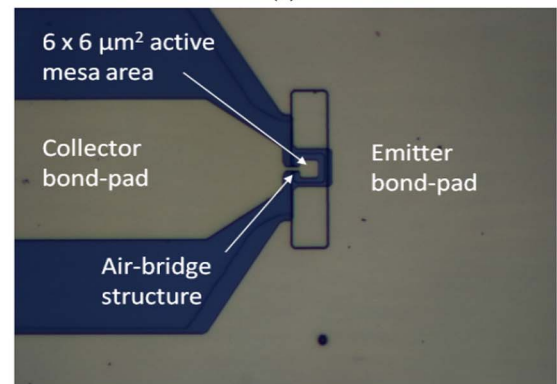
The active area or mesa is defined using a conventional wet etching. Since wet etching not only etches vertically, the mesa mask is designed with tolerances to compensate lateral etching. These tolerances are pre-defined with 0.25 μm , 0.50 μm , 1.0 μm and 2.0 μm from the edges of the top contacts. The Shipley S1805 positive resist is used to pattern the mesa area. A conventional non-selective Orthophosphoric-based wet etching with $\text{H}_3\text{PO}_4/\text{H}_2\text{O}_2/\text{H}_2\text{O}$ ratio of 3:1:50 is used. Based on 600 \AA per-minute etch rate, an etch depth of about 1 μm is achieved with 17 min immersion into the etchant. This depth is sufficient in order to reach the emitter layer for the preparation of bottom metal contact.

Just before the bottom metal contact process takes place, the sample underwent the second wet-etching process, similar to mesa step above in order to completely isolate neighbouring devices. Shipley S1813 resist is used to protect the bottom metal foot-print while allowing the rest of the sample to be etched about 300 nm into the buffer layer. It is noteworthy to mention that a total wet-etching time of 22 min for both step 2 and 3 would consequently form the suspended air-bridge structure by totally eliminating layers underneath the bridge.

Finally, the bottom metal contact is established on the emitter layer. This bottom metal contact is combined together with the bond pads (which sits on the buffer layer) to reduce processing steps. Similar metal scheme of AuGe/Ni/Au (50 nm/13 nm/380 nm) is employed to complete the electrical contacts. In order to produce good ohmic contacts,



(a)



(b)

Fig. 1. (a) SEM photograph of a complete $5 \mu\text{m} \times 5 \mu\text{m}$ active mesa GaAs/AlAs resonant tunneling diode and (b) actual microphotograph of a complete $6 \mu\text{m} \times 6 \mu\text{m}$ active mesa GaAs/AlAs resonant tunneling diode in this work.

the sample is then annealed at $420 \text{ }^\circ\text{C}$ for 90 s in a furnace with nitrogen (N_2) flow. The heat treatment causes metals to diffuse into the n-GaAs collector and emitter layers respectively, resulting in reduced contact resistances. This is termed the alloyed ohmic contact and the complete device is shown in Fig. 1(a) and (b).

3. Results and discussion

3.1. Contact resistance

For process control monitoring, the transmission line model (TLM) is used to extract the contact resistance, R_C values in order to determine the quality of the ohmic metal contacts. This method utilises 4-point measurement on TLM test structures built around the $15 \text{ mm} \times 15 \text{ mm}$ tile as in Fig. 2. The TLM structure is made of $100 \mu\text{m} \times 50 \mu\text{m}$ (width \times length) metal pads with 5 μm initial spacing. The spacing is increased by 5 μm until final spacing of 45 μm is reached. A constant current of 1 mA is passed between the first and the last metal pads by using two probes. Another two probes were used to measure the voltage drop between two adjacent pads. Then the total resistance is calculated by simply dividing the voltage (V) by the current (I). The two voltage probes then move to measure the voltage drop between two metal pads for the next spacing and so forth.

The graphical results for the TLM measurement of the top contact are displayed in Fig. 3(a) and (b) while Fig. 4(a) and (b) show the TLM measurement of the bottom metal contact. For TLM measurement, five TLM structures for top contact and four TLM structures for bottom contact were measured across the tile and the uniformity is excellent.

Download English Version:

<https://daneshyari.com/en/article/7150689>

Download Persian Version:

<https://daneshyari.com/article/7150689>

[Daneshyari.com](https://daneshyari.com)